The Planetary Science Journal, 5:109 (5pp), 2024 May https://doi.org/10.3847/PSJ/ad3b93
© 2024. The Author(s). Published by the American Astronomical Society.
OPEN ACCESS

# Probing the Rock Mass Fraction and Transport Efficiency inside Uranus Using $^{40}$Ar Measurements

Francis Nimmo[1], Jonathan Lunine[2], Kevin Zahnle[3], and Lars Stixrude[4]
[1] Department of Earth and Planetary Sciences, University of California Santa Cruz, 1156 High Street, Santa Cruz, CA 95064, USA; fnimmo@ucsc.edu
[2] Department of Astronomy, Cornell University Ithaca, NY 14853, USA
[3] Space Science Division, NASA Ames Research Center, Moffett Field, CA 94035, USA
[4] Department of Earth, Planetary and Space Sciences, UCLA Los Angeles, CA 90095, USA
*Received 2024 January 25; revised 2024 April 2; accepted 2024 April 5; published 2024 May 7*

## Abstract

The bulk of Uranus consists of a rock–ice core, but the relative proportions of rock and ice are unknown. Radioactive decay of potassium in the silicates produces $^{40}$Ar. If transport of argon from the core to the gaseous envelope is efficient, a measurement of $^{40}$Ar in the envelope will provide a direct constraint on the rock mass present (assuming a chondritic rock composition). The expected $^{40}$Ar concentrations in this case would be readily detectable by a mass spectrometer carried by a future atmospheric probe. For a given envelope concentration there is a trade-off between the rock mass present and the transport efficiency; this degeneracy could be overcome by making independent determinations of the rock mass (e.g., by gravity and seismology). Primordial $^{40}$Ar is a potential confounding factor, especially if $Ar/H_2$ is significantly enhanced above solar or if degassing of radiogenic $^{40}$Ar were inefficient. Unfortunately, the primordial $^{40}Ar/^{36}Ar$ ratio is very uncertain; better constraints on this ratio through measurement or theory would be very helpful. Pollution of the envelope by silicates is another confounding factor but can be overcome by a measurement of the alkali metals in the envelope.

*Unified Astronomy Thesaurus concepts:* Planetary interior (1248)

## 1. Introduction

The internal structure of Uranus consists of a gas envelope underlain by a more massive core of heavy elements (e.g., Helled et al. 2020). Although cosmochemical abundances suggest that this core must consist primarily of "rock" (silicates + iron) and "ice" (water, methane, etc.) (Stevenson 1985), the relative proportions of these two components is essentially unknown. This is because a mixture of rock plus hydrogen and helium has the same density as ice, and can thus substitute for it (Podolak et al. 1995). As a result, whether Uranus has a rock-rich or ice-rich interior is very uncertain (Teanby et al. 2020; Neuenschwander et al. 2024), as is the degree to which these two components are mixed (Helled & Fortney 2020).

Because of its high scientific interest, the Uranus system was identified by the recent Planetary Sciences and Astrobiology Decadal Survey as the top priority for the next Flagship mission (National Academies of Sciences 2023). Any such mission will certainly include determining Uranus's bulk structure as ones of its key objectives, and will likely include an atmospheric probe. The standard way to determine structure is by fitting the gravity field of the planet to an interior model that specifies the density with radius, and then inferring composition with the help of equations of state and temperature profiles. Such an approach by itself will not provide the accuracy needed to derive the rock-to-ice ratio unambiguously (Movshovitz & Fortney 2022).

In this paper we suggest another potential way of determining Uranus's rock abundance by measurements of Uranus's gaseous envelope. The noble gas $^{40}$Ar is produced by radioactive decay of $^{40}$K, which is typically hosted in silicates. Assuming that $^{40}$Ar is transported outwards efficiently from the core, a measurement of the envelope $^{40}$Ar concentration will then provide an estimate of the total mass of silicates present in Uranus. When combined with gravity measurements, constraints on the distribution of rock and ice may be obtained, as well as an estimate of the long-term transport rate between core and envelope. Determining this transport rate is important for understanding the luminosity and chemical mixing history of the planet (e.g., Chau et al. 2011; Helled et al. 2020). A very low rate might imply a stably stratified region or thermal boundary layer (Nettelmann et al. 2016; Vazan & Helled 2020; Scheibe et al. 2021) that would impede outwards transport while being potentially detectable via gravitational or ring seismology (see below).

The rest of this paper is organized as follows. In Section 2 we discuss $^{40}$Ar production and provide some first-order calculations. In Section 3 we discuss how much potassium is likely to be present in the rocky portion of Uranus, and in Section 4 we discuss the processes by which Ar transport to the outer envelope may occur. This section in particular highlights the current large uncertainties arising from our ignorance of argon's physical properties at the relevant $P$, $T$ conditions. Section 5 addresses the issue of primordial $^{40}$Ar, another area where further laboratory measurements would be very helpful. Section 6 briefly discusses the potential issue of envelope pollution (that is, some of the rock is stranded in the envelope) and Section 7 summarizes our findings.

Throughout this paper our notional picture of Uranus's structure is a simplified one: a gaseous, H-dominated envelope that is separate from and overlies a denser rock/ice core. While this picture may not be correct (e.g., there might be nonnegligible H in the deep interior), it is conceptually simple; more complex models are hard to justify given our current level of ignorance.

Original content from this work may be used under the terms of the Creative Commons Attribution 4.0 licence. Any further distribution of this work must maintain attribution to the author(s) and the title of the work, journal citation and DOI.

## 2. $^{40}$Ar Production

$^{40}$Ar is a noble gas isotope that is produced by radioactive decay of $^{40}$K (half-life 1.25 Gyr; e.g., Kaula 1999). Potassium is lithophile (found primarily in silicates) and moderately volatile, and is found in chondritic materials with a typical concentration of about 0.05 wt% (Palme & O'Neill 2014). Uranus contains an unknown mass of silicates, producing $^{40}$Ar over the age of the solar system.[5] The concentration of $^{40}$Ar in the atmosphere of Uranus therefore depends on the total rock mass, the initial K concentration in the rock, and the degree to which $^{40}$Ar has been transported outwards. Given the first two quantities, a measurement of atmospheric $^{40}$Ar constrains the degree to which the deep interior and the atmosphere are in communication. Although the use of $^{40}$Ar as a tracer of the degree of silicate outgassing to atmospheres is a familiar technique on the Earth and Venus (e.g., Namiki & Solomon 1998; Kaula 1999), to our knowledge it has not been proposed as a useful tool for giant planets before.

The chondritic concentration of potassium is 546 ppm (Palme & O'Neill 2014) and the present-day fraction of $^{40}$K is 0.0117 wt%. So the present-day chondritic concentration of $^{40}$K atoms $C_{40K}$ is 63.9 ppb, and this represents 8.3% of the initial concentration (given the 1.25 Gyr half-life and an assumed solar system age of 4.5 Gyr). Since the branching ratio of $^{40}$K atom decay to $^{40}$Ar is 0.105 (Kaula 1999), the concentration of $^{40}$Ar atoms $C_{40Ar}$ produced over the age of the solar system $t_0$ is then 74 ppb. If Uranus contained three Earth masses (3 $M_E$;$1.9 \times 10^{25}$ kg) of chondritic material, it would have produced $1.4 \times 10^{18}$ kg of $^{40}$Ar over the age of the solar system.

If all this $^{40}$Ar were mixed uniformly into a 1 $M_E$ envelope, the concentration (g g$^{-1}$) of $^{40}$Ar in the envelope would be $2.2 \times 10^{-7}$. More pertinently for determination by a mass spectrometer, assuming an envelope molar mass of 2.5, the number concentration (atoms atom$^{-1}$) would be $1.4 \times 10^{-8}$. For comparison, the predicted dynamic range of the Galileo Probe Mass Spectrometer (GPMS) was $10^8$, and the actual performance was better by a factor of a few (Niemann et al. 1996). A more modern space-qualified mass spectrometer, ROSINA on Rosetta, had a dynamic range 100 times larger (Balsiger et al. 2007). Argon should not condense as cloud particles or partition into other clouds in the Uranian atmosphere (Zahnle 2024). Thus, $^{40}$Ar present at our calculated concentrations should be readily detectable in Uranus's envelope by a future atmospheric probe carrying existing space-qualified mass spectrometers.

Figure 1 summarizes our calculations, showing the envelope $^{40}$Ar concentration as a function of the ratio of the (chondritic) rock core mass to the envelope mass. For our baseline Uranus case (above) we are assuming a rock core:envelope mass ratio of 3:1. For Jupiter and Saturn, the total core masses are roughly 7–25 $M_E$ (Wahl et al. 2017) and 17 $M_E$ (Mankovich & Fuller 2021), respectively, but the envelopes are more like 300 and 100 $M_E$. For a detection limit of $3 \times 10^{-9}$ (dotted line), a Uranus-like core:envelope mass ratio of 1:1 or 3:1 would still produce detectable $^{40}$Ar, assuming complete outgassing. Conversely, for Jupiter the expected signature is well below the detection limit, thanks to the much greater dilution in the massive H–He envelope. This is consistent with the nondetection of $^{40}$Ar by the Galileo probe (Niemann et al. 1996).

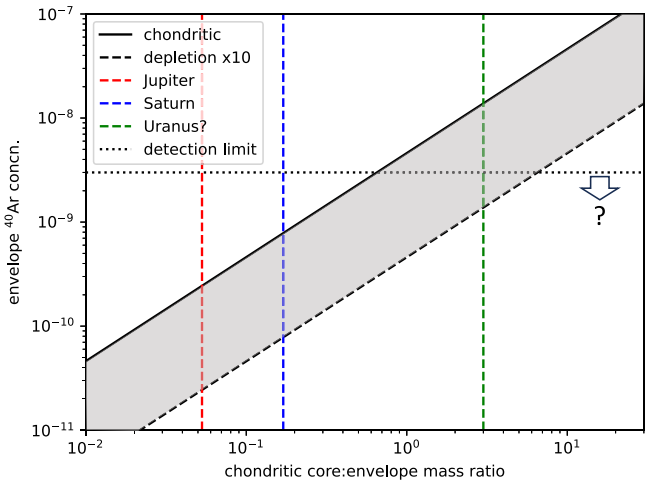


**Figure 1.** Envelope concentration (in atoms atom$^{-1}$) of radiogenic $^{40}$Ar as a function of rock core:envelope mass ratio, assuming a core argon concentration ranging from CI chondritic to 10% of the chondritic value (gray shaded zone). Our baseline Uranus (green dashed line) assumes a 3 $M_E$ chondritic core and a 1 $M_E$ envelope. Detection limit is based on a GPMS-like instrument (see text), with the strong possibility that what is flown will have better sensitivity by a significant factor (downward arrow).

Thus, as long as there is enough potassium inside Uranus, and as long as transport of $^{40}$Ar from the deep interior to the surface is efficient, then it ought to be detectable in Uranus's envelope. Conversely, a low or absent $^{40}$Ar concentration would provide information on Uranus's bulk composition and/or the planet's ability to transport material outwards from the deep interior.

## 3. How Much Potassium?

The total amount of potassium present depends on two factors: how much rock is present in Uranus, and what the concentration of potassium in the rock is.

The rock mass fraction of Uranus is very uncertain, because of the density degeneracy between ices and rock + H/He (Podolak et al. 1995). Because of this same degeneracy, the H/He envelope mass of Uranus is also uncertain. Empirical Uranus models suggest an envelope mass fraction of 0.08–0.25, or 1.1–3.4 $M_E$ (Helled et al. 2010).

Some models of the internal structure of Uranus suggest very low rock:ice mass ratios. For instance, in the three-layer models of Nettelmann et al. (2013), ice is 19–35 times more abundant than rock. However, as noted by Helled & Fortney (2020), such a high ratio is not found in any solar system object, and models in which rock and ice are mixed, rather than fully separated, tend to increase the rock:ice ratio. Other authors argue for a rock-rich Uranus on the basis of the observed envelope concentrations of D/H and CO (Feuchtgruber et al. 2013; Teanby et al. 2020). Unfortunately, without additional compositional constraints, determining the rock:ice ratio from existing geophysical data is essentially impossible (Movshovitz & Fortney 2022).

Solar condensation models suggest that the primordial rock:ice mass ratio should be in the range 1:2 to 1:3 (e.g., Podolak et al. 1995; Lodders 2003). For a total core mass of 12 $M_E$, this range implies a rock core mass range of 3–4 $M_E$. Kuiper Belt objects have a rock:ice mass ratio of about 2:1 (Bierson &

[5] In principle $^4$He (which is produced by decay of U and Th) could be used in addition to $^{40}$Ar. However, there is also a primordial $^4$He component that will completely overwhelm the radiogenic helium contribution.

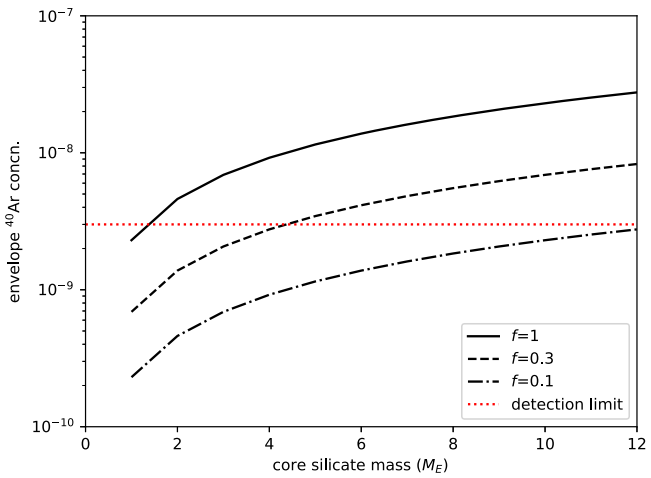


**Figure 2.** Concentration of radiogenic $^{40}$Ar in the envelope as a function of chondritic core rock mass. Here $f$ is the transport factor and we assume a 2 $M_E$ envelope. The red dashed line is a notional detection threshold.

Nimmo 2019), and this is roughly the rock:ice ratio deduced for Uranus based on D/H measurements by Feuchtgruber et al. (2013). In this case, 8 $M_E$ or more of silicates could be present. Based on existing data, we cannot confidently assign a total silicate mass to Uranus—which is why the $^{40}$Ar measurements are interesting.

The terrestrial planets are depleted in potassium and other moderately volatile elements (MVEs) relative to chondritic. In the case of potassium, a good proxy for the degree of depletion is the K/U ratio, because K and U have similar chemical affinities but U is refractory. The terrestrial planets have a K/U ratio roughly a factor of 7 lower relative to chondritic; for the Moon, this factor is more like 30 (McCubbin et al. 2012). This depletion is most likely due to incomplete condensation (Hu et al. 2023), though heating and loss during accretion may also play a role (Sossi et al. 2019). At plausible locations of Uranus in the protoplanetary disk (i.e., beyond 10 au), incomplete condensation of MVEs is very unlikely because disk temperatures are too low (Chambers 2009). Heating mechanisms such as $^{26}$Al decay might drive off MVEs in planetesimals prior to their addition to Uranus, but the density distribution of Kuiper Belt objects suggest that they only accreted after $^{26}$Al had decayed (Bierson & Nimmo 2019). Accordingly, we regard depletion of K in silicates in the core of Uranus as unlikely, and conclude that assuming a chondritic K concentration is reasonable.

After CI chondrites, the most volatile-rich class is the CMs, which have a potassium concentration of 380 ppm (Braukmüller et al. 2018), i.e., a 30% depletion relative to CI. This factor is probably a reasonable indication of the uncertainty in the "chondritic" concentration assumed; below we will continue to assume CI values.

## 4. Transport

Assuming for the moment that the silicates are contained within Uranus's core, the $^{40}$Ar concentration in the envelope then depends on the efficiency with which they are transported away from where they are produced. We will introduce a transport efficiency factor $f$, which simply gives the fraction of all $^{40}$Ar produced that reaches the envelope, assuming the latter to be well mixed.

Figure 2 shows the resulting envelope concentration as a function of the mass of chondritic silicates in the core, and $f$. A degassing efficiency of $f = 0.1$ would result in a barely detectable signal for a GPMS-like spectrometer if the entire core (12 $M_E$) were silicates, but one easily detectable with ROSINA sensitivity. Conversely, efficient degassing ($f = 1$) would provide a detectable signal down to rock core masses of 1 $M_E$ or less. The most important point about this figure is that it illustrates a trade-off: a measurement of envelope $^{40}$Ar can be explained by many different combinations of core mass and transport factor $f$. This degeneracy could be broken by making use of other measurements, such as gravity (see below).

We will next discuss the physical processes that go into the efficiency factor $f$. As will become clear, current uncertainties about the internal state of Uranus prohibit any definitive conclusions. Nonetheless, for $^{40}$Ar to be detectable in the envelope, it must (1) escape from the original site of production in a silicate grain; and (2) migrate upwards through the rock–ice core to the envelope. Neither of these processes is guaranteed to happen. It might even be that the envelope itself is not well mixed.

A major difficulty is our uncertainty in the temperature structure, and thus the state, of the Uranian interior. Depending on whether the interior is stably stratified or not, central temperatures can range from 7000 K to almost 30,000 K (Vazan & Helled 2020; Neuenschwander et al. 2024). At least for the colder end-members, it seems likely that silicates inside Uranus will be solid (Millot et al. 2015; González-Cataldo et al. 2016). In this case Ar would have to diffuse to the edges of silicate grains. Diffusivity follows an Arrhenius relationship, and near the melting point diffusivities of noble gases (except He) in silicate glasses are typically $10^{-11}$–$10^{-9}$ m$^2$ s$^{-1}$ (Carroll & Stolper 1991). Over 4 Gyr the diffusion distance is then of order 1–10 km. A solid, monolithic, impermeable silicate core would thus permit almost no $^{40}$Ar to migrate. However, the presence of melt, fluids, or grain boundaries would invalidate this argument, since transport along grain boundaries is very rapid (Kaula 1999). Small silicate particles dispersed in a fluid medium (e.g., superionic water) would permit rapid $^{40}$Ar escape. Given the uncertainties, we cannot predict the value of $f$ based on first-principles arguments concerning transport within the silicates.

Transport of Ar atoms through the "ice" part of the core will depend on its state, the state of the ice, and the density contrast between Ar and ice. If a condensed phase of argon forms—which is not guaranteed—a positive buoyancy contrast will make upwards transport more likely.

There are only limited data on the high-pressure behavior of Ar. At 100 GPa, its melting temperature is in the range 3500–4000 K (Boehler et al. 2001). Whether it will be solid at central core conditions (~600 GPa) depends on the poorly known temperature structure (see above). The density of solid Ar at 100 GPa and room temperature is about 5000 kg m$^{-3}$ (Dewaele et al. 2021). This density is comparable to the expected central core densities (Vazan & Helled 2020); it does not take into account the effect of the high temperatures expected, which is probably minor (Jephcoat 1998). Accordingly, it is difficult to determine whether Ar would have positive buoyancy relative to the materials surrounding it in the core.

It is often assumed that the ice is in a superionic liquid state, and thus adiabatic and convective (Helled & Fortney 2020). If so, then argon—irrespective of its density—could be entrained

in upwellings and transported to shallower depths where it becomes gaseous. However, it is possible that the deeper parts of the ice are solid (Stixrude et al. 2021), in which case the transport timescale would be much longer. In addition, stably stratified layers (Vazan & Helled 2020) would impede upwards transport unless the Ar were buoyant. Such layers are known to exist at both Jupiter and Saturn (Helled & Stevenson 2024) and could in principle be detected using other techniques, especially seismology (A'Hearn et al. 2022) or measurement of the tidal response (Idini & Stevenson 2022). At present, the rates at which mass and energy are transferred across these stably stratified regions is very poorly understood.

Another way of interrupting $^{40}$Ar transport would be if $^{40}$Ar partitions preferentially into nongas species. For instance, $^{40}$Ar might partition into superionic water rather than H/He gas. The presence of such a water layer might be inferred from other techniques, including those mentioned above and also magnetic observations (Redmer et al. 2011).

One further but highly speculative complication is that K might partition into an iron core, if one exists. At Earth-like pressures, such partitioning does not appear to be important (Xiong et al. 2018), but the partitioning behavior of K at higher pressures is currently unknown.

## 5. Primordial $^{40}$Ar

So far, we have assumed that all $^{40}$Ar produced is from radioactive decay of $^{40}$K. In fact, some $^{40}$Ar is likely primordial and thus would need to be accounted for prior to drawing conclusions about rock abundance and the efficiency of outgassing.

There are two approaches to determining the primordial $^{40}$Ar abundance. The first is to look for the lowest (i.e., least radiogenic) $^{40}$Ar/$^{36}$Ar ratios in K-poor minerals in primitive meteorites. Göbel et al. (1978) found that $^{40}$Ar/$^{36}$Ar was highly variable. After correcting for the blank, they interpreted their lowest measured $^{40}$Ar/$^{36}$Ar ratio of $1.17 \pm 0.2 \times 10^{-3}$ as an upper bound of $2.9 \pm 1.7 \times 10^{-4}$. In an abstract, Murty & Ghosh (2015) suggested that with a different blank correction the upper bound could be reduced to $1.1 \times 10^{-4}$.

The second approach is to model $^{40}$Ar nucleosynthesis. Beer & Penzhorn (1987) used a theoretical description of *s*-process nucleosynthesis to derive a range of $8.4 \times 10^{-5} < ^{40}\mathrm{Ar}/^{36}\mathrm{Ar} < 2.9 \times 10^{-4}$. They favored the higher ratio because in this case their model gave a good match to solar $^{40}$K/Si, while the lower $^{40}$Ar/$^{36}$Ar ratio implied $^{40}$K/Si that was twice solar. Macklin et al. (1989) agreed with the calculations, but they favored the smaller $^{40}$Ar/$^{36}$Ar as more consistent with other aspects of *s*-process nucleosynthesis.

Although rather sparse, these constraints thus suggest a primordial $^{40}$Ar/$^{36}$Ar ratio in the range of $1–3 \times 10^{-4}$. How would the presence of primordial $^{40}$Ar affect our conclusions?

To address this, we assume that the final mass of $^{40}$Ar in the atmosphere consists of a degassed, radiogenic component and a primordial component ($^{36}$Ar is solely primordial). We take the baseline primordial $^{40}$Ar/$^{36}$Ar ratio to be $1.5 \times 10^{-4}$.

The ratio of radiogenic $^{40}$Ar to primordial $^{36}$Ar may be written as $^{40}\mathrm{Ar}^*/\mathrm{H} \times \mathrm{H}/^{36}\mathrm{Ar}$, where here an asterisk denotes a radiogenic species. The solar mass ratio $^{36}$Ar/H is $8.33 \times 10^{-5}$ (Lodders 2021), and we anticipate that Uranus's envelope will be enriched in volatiles relative to solar by a factor *r*. From Section 2, with a core-to-envelope mass ratio of 3:1, the $^{40}\mathrm{Ar}^*/\mathrm{H}$ mass ratio is $2.2 \times 10^{-7}$. In this case, the resulting $^{40}\mathrm{Ar}^*/^{36}\mathrm{Ar}$ is $2.6 \times 10^{-3}/r$.

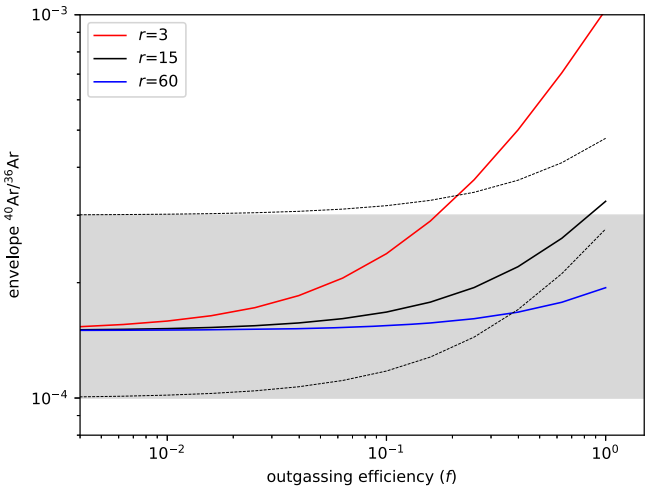


**Figure 3.** Envelope ratio of $^{40}$Ar/$^{36}$Ar taking the effect of primordial $^{40}$Ar into account (see text). The thick solid lines plot the $^{40}$Ar/$^{36}$Ar ratio for three different values of the enhancement factor *r* with $\xi = 1.5 \times 10^{-4}$. The gray shaded box denotes the uncertainty in the primordial $^{40}$Ar/$^{36}$Ar ratio $\xi$ and the thin dashed black lines show the effect on the $r = 15$ model of using these upper and lower bounds. Here a rock core:envelope mass ratio of 3:1 is assumed.

Sromovsky et al. (2011) retrieve Uranus $CH_4$ molar mixing ratios between 2.3% and 4.9%, with 4% their preferred value. The apparent C/H enrichment over the protosolar C/H ratio (Lodders 2021) is large, of order $70 \pm 30$. Jupiter's Ar may be 20%–40% less enriched than C (Atreya et al. 2020), using the protosolar values from Lodders (2021). So one might expect an Ar enrichment *r* at Uranus of up to 60, with large uncertainties.

Let $\xi$ denote the primordial $^{40}$Ar/$^{36}$Ar ratio. With *r* and *f* as defined above, the envelope's $^{40}$Ar/$^{36}$Ar ratio can be approximated by

$$\frac{^{40}\mathrm{Ar}}{^{36}\mathrm{Ar}} = \xi + 8.8 \times 10^{-4} \frac{M_{\mathrm{rock}}\, f}{M_{\mathrm{env}}\, r}. \quad (1)$$

In Figure 3 we plot the total $^{40}$Ar/$^{36}$Ar ratio as a function of outgassing efficiency *f* for three different values of *r*.

The figure assumes a fixed rock core/envelope mass ratio $M_{\mathrm{rock}}/M_{\mathrm{env}}$ of 3. Solid lines assume an arbitrary choice of $\xi = 1.5 \times 10^{-4}$. The horizontal gray band indicates upper and lower bounds on the primordial $^{40}$Ar/$^{36}$Ar ratio; a value above this range would be unambiguous indications of radiogenic $^{40}$Ar. Higher values of *r* make it harder to detect radiogenic $^{40}$Ar, because there is more primordial $^{40}$Ar. There is thus a trade-off between *f* and *r* in terms of whether a $^{40}$Ar excess can be detected. Figure 3 illustrates that it would be extremely valuable to reduce existing uncertainties in the primordial $^{40}$Ar/$^{36}$Ar ratio.

## 6. Envelope Pollution

So far we have assumed that all the silicates reside in the deep interior of Uranus. In reality, it is possible that the envelope contains a nonnegligible fraction of heavy elements. These could either have been deposited as part of the original accretion process (Hasegawa 2022) or added after planet formation was complete. In either case, whether such heavy elements could be retained in the envelope over billions of years depends strongly on the details of the delivery process

(Pinhas et al. 2016; Valletta & Helled 2019) and the envelope dynamics. With envelope pollution, none of the complications discussed in Section 4 apply: the $^{40}$Ar produced will be promptly mixed into the envelope. However, this Ar does not indicate anything about transport from the deep interior. To remove this confounding effect, it would be important to look for enrichments over solar of rock-related elements (such as potassium and other alkali metals) in the envelope with an atmospheric probe or a microwave radiometer.

Observations of exoplanets might also provide clues. Sodium is a moderately volatile element that is chemically very similar to potassium, and is readily detectable by spectroscopy (e.g., Nikolov et al. 2018). If young Uranus-class exoplanets do not show strong Na spectral features, that would suggest that envelope pollution is not important (at least in general), and vice versa.

## 7. Conclusions

The idea of using $^{40}$Ar as a proxy for Uranus's rock abundance and interior-atmospheric communication is novel (to the best of our knowledge). To be most useful, one would want to be able to determine both the transport factor $f$ and the core rock mass. However, as Figure 2 illustrates, a measurement of $^{40}$Ar alone results in a degeneracy between these two parameters. Breaking this degeneracy to determine $f$ would require independent measurements of the rock mass fraction (e.g., using gravity and seismology) and measurements of envelope concentrations of alkali metals. A future Uranus Orbiter and Probe should be able to accomplish these goals.

Figures 1 and 2 suggest that there should be enough radiogenic $^{40}$Ar to be detectable. However, primordial $^{40}$Ar is likely to complicate this picture (Figure 3) so that a measurement of the $^{40}$Ar/$^{36}$Ar ratio would also be very important. Interpretation of this value will hinge on better knowledge of the primordial $^{40}$Ar/$^{36}$Ar ratio than we have at present.

In anticipation of a future mission, both theoretical and experimental studies could be performed now to improve the eventual prospects for a successful measurement. These include: better measurements or updated nucleosynthesis theory to determine the primordial $^{40}$Ar/$^{36}$Ar ratio (Section 5); a better determination of the physical characteristics of Ar at the relevant $P$, $T$ conditions (Section 4); and further theoretical studies of both envelope pollution (Section 6) and transport across stably stratified layers (Section 4). Such studies would be highly desirable while we wait for a mission.

## Acknowledgments

We thank the organizers of the KISS workshop on the interior of Uranus for stimulating discussions, Guillaume Avice and two anonymous reviewers for helpful comments. J.L. acknowledges support from the JPL Distinguished Visiting Scientist program.

## ORCID iDs

Francis Nimmo https://orcid.org/0000-0003-3573-5915
Jonathan Lunine https://orcid.org/0000-0003-2279-4131
Kevin Zahnle https://orcid.org/0000-0002-2462-4358
Lars Stixrude https://orcid.org/0000-0003-3778-2432

## References

Atreya, S. K., Hofstadter, M. H., In, J. H., et al. 2020, SSRv, 216, 18
A'Hearn, J. A., Hedman, M. M., Mankovich, C. R., Aramona, H., & Marley, M. S. 2022, PSJ, 3, 194
Balsiger, H., Altwegg, K., Bochsler, P., et al. 2007, SSRv, 128, 745
Beer, H., & Penzhorn, R.-D. 1987, A&A, 174, 323
Bierson, C., & Nimmo, F. 2019, Icar, 326, 10
Boehler, R., Ross, M., Söderlind, P., & Boercker, D. B. 2001, PhRvL, 86, 5731
Braukmüller, N., Wombacher, F., Hezel, D. C., Escoube, R., & Münker, C. 2018, GeCoA, 239, 17
Carroll, M., & Stolper, E. 1991, GeCoA, 55, 211
Chambers, J. 2009, ApJ, 705, 1206
Chau, R., Hamel, S., & Nellis, W. J. 2011, NatCo, 2, 203
Dewaele, A., Rosa, A. D., Guignot, N., et al. 2021, NatSR, 11, 15192
Feuchtgruber, H., Lellouch, E., Orton, G., et al. 2013, A&A, 551, A126
Göbel, R., Ott, U., & Begemann, F. 1978, JGR, 83, 855
González-Cataldo, F., Davis, S., & Gutiérrez, G. 2016, NatSR, 6, 26537
Hasegawa, Y. 2022, ApJ, 935, 101
Helled, R., Anderson, J. D., Podolak, M., & Schubert, G. 2010, ApJ, 726, 15
Helled, R., & Fortney, J. J. 2020, RSPTA, 378, 20190474
Helled, R., Nettelmann, N., & Guillot, T. 2020, SSRv, 216, 38
Helled, R., & Stevenson, D. J. 2024, AGUA, 5, e2024AV001171
Hu, Y., Moynier, F., & Yang, X. 2023, E&PSL, 620, 118319
Idini, B., & Stevenson, D. J. 2022, PSJ, 3, 89
Jephcoat, A. P. 1998, Natur, 393, 355
Kaula, W. M. 1999, Icar, 139, 32
Lodders, K. 2003, ApJ, 591, 1220
Lodders, K. 2021, SSRv, 217, 44
Macklin, R., Winters, R., & Schmidt, D. 1989, A&A, 216, 109
Mankovich, C. R., & Fuller, J. 2021, NatAs, 5, 1103
McCubbin, F. M., Riner, M. A., Vander Kaaden, K. E., & Burkemper, L. K. 2012, GeoRL, 39, L09202
Millot, M., Dubrovinskaia, N., Černok, A., et al. 2015, Sci, 347, 418
Movshovitz, N., & Fortney, J. J. 2022, PSJ, 3, 88
Murty, S. V. S., & Ghosh, S. 2015, Annual Meeting of the Meteoritical Society, 78, 5024
Namiki, N., & Solomon, S. C. 1998, JGR, 103, 3655
National Academies of Sciences 2023, Origins, Worlds and Life: Planetary Science and Astrobiology in the Next Decade (Washington, DC: The National Academies Press),
Nettelmann, N., Helled, R., Fortney, J., & Redmer, R. 2013, P&SS, 77, 143
Nettelmann, N., Wang, K., Fortney, J. J., et al. 2016, Icar, 275, 107
Neuenschwander, B. A., Müller, S., & Helled, R. 2024, arXiv:2401.11769
Niemann, H. B., Atreya, S. K., Carignan, G. R., et al. 1996, Sci, 272, 846
Nikolov, N., Sing, D. K., Fortney, J. J., et al. 2018, Natur, 557, 526
Palme, H., & O'Neill, H. 2014, in Treatise on Geochemistry, Vol. 2, ed. A. M. Davis (Amsterdam: Elsevier)
Pinhas, A., Madhusudhan, N., & Clarke, C. 2016, MNRAS, 463, 4516
Podolak, M., Weizman, A., & Marley, M. 1995, P&SS, 43, 1517
Redmer, R., Mattsson, T. R., Nettelmann, N., & French, M. 2011, Icar, 211, 798
Scheibe, L., Nettelmann, N., & Redmer, R. 2021, A&A, 650, A200
Sossi, P. A., Klemme, S., O'Neill, H. S. C., Berndt, J., & Moynier, F. 2019, GeCoA, 260, 204
Sromovsky, L., Fry, P., & Kim, J. H. 2011, Icar, 215, 292
Stevenson, D. J. 1985, Icar, 62, 4
Stixrude, L., Baroni, S., & Grasselli, F. 2021, PSJ, 2, 222
Teanby, N., Irwin, P., Moses, J., & Helled, R. 2020, RSPTA, 378, 20190489
Valletta, C., & Helled, R. 2019, ApJ, 871, 127
Vazan, A., & Helled, R. 2020, A&A, 633, A50
Wahl, S. M., Hubbard, W. B., Militzer, B., et al. 2017, GeoRL, 44, 4649
Xiong, Z., Tsuchiya, T., & Taniuchi, T. 2018, JGRB, 123, 6451
Zahnle, K. 2024, PSJ, 5, 73